Combining Extrapolated Electron Localization Functions and Berlin's Binding Functions for the Prediction of Dissociative Electron Attachment

Charlotte Titeca,[1, 2, a)] Thomas-Christian Jagau,[1] and Frank De Proft[2]

[1)] *Division of Quantum Chemistry and Physical Chemistry, Department of Chemistry, KU Leuven, Leuven, Belgium*

[2)] *Research Group of General Chemistry (ALGC), Vrije Universiteit Brussel, Brussel, Belgium*

(Dated: 15 January 2024)

Computational study of electronic resonances is still a very challenging topic, with the phenomenon of dissociative electron attachment (DEA) being one of the multiple features worth investigating. Recently, we extended the charge stabilization method from energies to properties of conceptual density functional theory and applied this to metastable anionic states of ethene and chlorinated ethene derivatives, to study the DEA mechanism present in these compounds. We now present an extension to spatial functions, namely the electronic Fukui function and the electron localization function. The results of our analysis show that extrapolated spatial functions are relevant and useful for more precise localization of the unbound electron. Furthermore, we report for the first time the combination of the electron localization function with Berlin's binding function for these challenging electronic states. This promising methodology allows for accurate predictions of when and where DEA will happen in the molecules studied and provides more insight into the process.

[a)] charlotte.titeca@kuleuven.be

I. INTRODUCTION

Electronic resonances are widespread in nature and involved in numerous processes. They are characterized by the presence of unbound electrons, responsible for the metastable nature of these species. The most frequently observed decay mechanisms are loss of a single electron (autodetachment) and fragmentation without electron loss (dissociative electron attachment, DEA).[45] The latter process is of much interest, since it allows for bond breaking caused by simple attachment of an electron. The resulting fragments are most often a stable anion and a radical organic fragment.[46] DEA to halogenated ethene derivatives has frequently been the subject of investigation, especially to chlorinated ethenes, which produces chloride anions. These compounds are models for many chlorinated unsaturated organic molecules, such as chlorobenzenes or the biologically relevant chlorouracil. Burrow and co-workers[47] were the first to postulate a mechanism for DEA to chloroethenes, based on their own observations and those reported in earlier publications. By performing both electron transmission spectroscopy on the anionic species and Hartree-Fock calculations on the neutral molecules, they found multiple resonance states of different symmetries (Π and Σ) and obtained energies for them. Furthermore, the formation of the lowest-energy resonance state, which is of Π symmetry, coincided with an observed peak of chloride production. Based on symmetry arguments however, DEA should take place starting from a Σ anionic state. They thus proposed that the initially formed Π state anions would be subject to out-of-plane distortion followed by crossover to a Σ state, which eventually leads to fragmentation.[47]

Many researchers have since studied the process, both experimentally and computationally. Computational investigations face the issue that unbound electrons cannot be described by conventional Hermitian quantum-chemical methods designed for bound states. The lowest-energy SCF solution for an anionic electronic resonance consists of an isolated electron placed in the most diffuse orbital, as far away from the molecule as possible.[48] Also, higher-lying states can usually not be associated with the resonance. Rather, the resonance character is spread over several states.[49] One way to overcome this problem is the use of non-Hermitian quantum chemistry. Here, the resonance state is turned into a single square-integrable state with complex Siegert energy[50]

$$E_{\text{res}} = E_R - i\Gamma/2. \tag{1}$$

The real part E_R is interpreted in the usual way as the energy of the state, whereas the imaginary part Γ, known as the width, is inversely proportional to the lifetime τ of the resonance state. Frequently used non-Hermitian methods comprise inclusion of complex basis functions[51] and addition of a complex absorbing potential to the Hamiltonian.[52–54] For more details, see for instance references 49 and 55. Recent efforts to use non-Hermitian quantum chemistry for studying chloroethene anions almost all made use of a complex absorbing potential. These consist of a wide variety of calculations, such as scanning along the complex potential energy surface to locate the exceptional points between the different resonance states,[56] using the analytical gradients for determining the minimum-energy crossing points between the neutral species and the resonances,[57] and the exceptional points,[58] and performing *ab initio* molecular dynamics to probe the geometric changes occurring during DEA.[59] These studies all confirmed the out-of-plane distortion as well as cross-over from a state of mainly Π character to a state of predominant Σ character near the exceptional points. Furthermore, from the obtained resonance widths the competition between autodetachment and DEA could be demonstrated.

A second set of methods for computational study of electronic resonances consists of making minimal modifications such that the conventional methods are still applicable. Recently, we employed this for investigating the same set of chlorinated ethene anions.[60] We made use of the so-called charge stabilization method, proposed by Nestmann and Peyerimhoff, which consists in introducing an additional attractive potential aimed at binding the unbound electron.[61] This is achieved by scaling all nuclear charges in the molecule by a factor $(1 + \lambda)$. Originally, charge stabilization was applied only for the calculation of total energies and electron affinities. We showed that the method is also applicable to properties from conceptual density functional theory. For each of the chlorinated ethene derivatives, we detected a Π and a Σ resonance state. From the evaluation of electronic[62,63] and nuclear Fukui functions,[64] we confirmed that the bond dissociation most likely occurs from the Σ anionic state.[60] We also aimed at finding a method for predicting when and where DEA could happen. However, this proved not yet possible from our previous results. We obtained large forces in the Π state on the carbon-carbon double bond but cleavage of this bond has never been observed experimentally. These forces are nevertheless in agreement with the findings from Benda and Jagau, who report that the equilibrium geometry of the Π anionic state has an elongated carbon-carbon bond as compared to the neutral molecule.[57] In the

present work, we use only the equilibrium structures of the neutral molecules, avoiding the need to optimize the structure of the metastable anions.

We report here the application of two additional functions used in the study of chemical reactivity. The first one is the electron localization function (ELF).[65–68] Its interpretation fits the intuitive idea of electron pairs forming bonds or remaining as lone pairs. For that reason, it is frequently used in a variety of theoretical studies, for instance to probe evolution of chemical bonds when the electronic state changes[69] or to localize the unpaired electron upon formation of a radical.[69,70] It is even possible to perform topological analysis of ELF and deduce conclusions about bond orders,[71] similarly to the analysis of the electron density. In this research however, we limit ourselves to localizing the excess electron in the studied anionic resonance states.

The second function that we employ, is Berlin's binding function (BBF).[72,73] Berlin developed this function to probe binding regions in diatomic molecules. These are regions where the presence of negative charge would generate forces that hold the nuclei together.[72] Multiple formulas have been proposed for obtaining the binding regions in polyatomic molecules,[73,74] the one by Wang and Peng[73] being the most used. BBF can be employed to study the influence of electron density changes on the molecular geometry. Berlin stated that addition of electron density in the binding regions of a diatomic molecule will cause the bond to shorten, while addition in the anti-binding regions will result in bond stretching.[72] This is now referred to as "Berlin's theorem", and is valid for polyatomic molecules as well. An alternative definition was given by Yonezawa and co-workers, who used the terms "accelerating" and "resisting": electron density in the accelerating region creates forces that accelerate nuclear rearrangement, while forces resulting from density in the resisting region will facilitate resistance against nuclear rearrangement.[74] Nonetheless, the definition by Berlin remains most used. Practically, it is most often investigated by considering the combination of BBF and a density-derived function that displays changes in electron density. Examples of such studies include prediction of Jahn-Teller distortions by combining BBF with the electronic Fukui function[75], and identification of bond breaking and formation events during a reaction, where BBF was used together with the derivative of the electron density with respect to a reaction coordinate.[76] Here, we report the use of ELF in combination with BBF. Using this, we also develop a method for predicting the occurence of

DEA, which we believe will be useful for the study of not only chloroethenes but many other compounds as well.

II. THEORETICAL CONSIDERATIONS

A. Charge stabilization method and procedure

We applied the charge stabilization method proposed by Nestmann and Peyerimhoff.[61] Only a short overview of the employed procedure will be given here; for a more detailed explanation, we refer the reader to our earlier work.[60] The resonance state is stabilized by an additional Coulomb field, created by scaling the nuclear charges in the molecule by a factor $(1 + \lambda)$, with $\lambda \geq 0$. For increasing values of λ, both the neutral compound and the metastable anionic state experience stabilization, however this stabilization is stronger for the anion. From a certain λ on, the anion is lower in energy than the neutral state, meaning that all electrons are bound. The data points associated with the stable valence anionic state can be extrapolated to $\lambda = 0$ by fitting a quadratic curve, and the intercept serves as an estimate of the studied property for the unstabilized resonance state. One should, however, check for the occurrence of diffuse continuum-like anionic states and make sure these are excluded from the extrapolation.[77,78]

Up until now, we had applied the procedure only to global properties: the electron affinity, the atom-condensed electronic Fukui function, the nuclear Fukui function and the position and value of the electron density at the bond critical points.[60] We now extend this to the extrapolation of spatial functions, more specifically the electronic Fukui function and the electron localization function. The procedure is very similar to the previous one. The spatial function of interest is obtained for various values of λ, each of these data sets is saved in a separate cube file. The same grid parameters must be used for all cube files. Subsequently, the extrapolation is applied to each grid point separately and the intercepts are collected in a new extrapolated cube file.

B. Electronic Fukui function

The theory behind the electronic Fukui function was explained in detail in our earlier manuscript, where we reported the application of the atom-condensed electronic Fukui function to anionic resonances. In the present work we used the function without condensing it onto the atoms. In the following, we provide only a short recapitulation.

The electronic Fukui function was introduced by Parr and Yang[62,63] and can be obtained as the mixed second derivative of the energy with respect to the number of electrons N and the external potential $v(\mathbf{r})$:

$$f(\mathbf{r}) = \frac{\partial^2 E}{\partial N \delta v(\mathbf{r})} = \left(\frac{\partial \rho(\mathbf{r})}{\partial N}\right)_{v(\mathbf{r})}. \tag{2}$$

The second equality results from $\rho(\mathbf{r}) = (\delta E/\delta v(\mathbf{r}))_N$.[62] This function shows regions that are favored in the attack of a reagent. Since we study processes in which the number of electrons increases, we are mostly interested in the right-hand-side derivative $f^+(\mathbf{r})$ with respect to N (indicated by the superscript "+"). This function specifically shows the regions favored by nucleophilic attack, i.e. when the considered molecule behaves as an electrophile. Therefore, $f^+(\mathbf{r})$ is also known as the electrophilic Fukui function. The derivative in Eq. 2 assumes a fractional number of electrons, which is in practice hard to achieve. Consequently, $f^+(\mathbf{r})$ is commonly approximated using a finite difference. The formula used in this research then becomes

$$f^+(\mathbf{r}) = \rho_{N_0+1}(\mathbf{r}) - \rho_{N_0}(\mathbf{r}) \tag{3}$$

where N_0 indicates the number of electrons in the neutral molecule. The electronic Fukui function can also be used to find regions of increased or decreased density due to a changing number of electrons. Upon assuming the "frozen core approximation" (the orbitals do not relax upon changing the number of electrons) and within Hartree-Fock or density functional theory, $f^+(\mathbf{r})$ can be regarded as the electron density purely due to the lowest unoccupied molecular orbital (LUMO) of the neutral species, or due to the highest occupied molecular orbital (HOMO) of the anionic species:[62]

$$\begin{aligned} f^+(\mathbf{r}) &\approx \rho_{N_0,\mathrm{LUMO}}(\mathbf{r}) = |\phi_{N_0,\mathrm{LUMO}}|^2 \\ &\approx \rho_{N_0+1,\mathrm{HOMO}}(\mathbf{r}) = |\phi_{N_0+1,\mathrm{HOMO}}|^2. \end{aligned} \tag{4}$$

C. Electron localization function

Bader and Stephens pointed out that electron localization is related to parallel-spin pair probability and the localization of Fermi holes.[79] Becke and Edgecombe used this argument to derive an orbital-independent measure of localization, starting from this pair probability.[65] The conditional pair probability $P^{\sigma\sigma}_{\text{cond}}(1,2)$ of finding a second electron ("2") near a reference electron ("1") of same spin σ is defined as

$$P^{\sigma\sigma}_{\text{cond}}(1,2) = \rho_\sigma(2) - \frac{|\rho^\sigma_1(1,2)|^2}{\rho_\sigma(1)}, \tag{5}$$

where $\rho_\sigma(x)$ represents the spin-density resulting from electron x ($x = 1, 2$), and $\rho^\sigma_1(1,2)$ the σ-spin one-electron density matrix of the Hartree-Fock or Kohn-Sham determinant:

$$\rho^\sigma_1(1,2) = \sum_i^\sigma \phi^*_i(1)\,\phi_i(2)\,. \tag{6}$$

When electron 2 approaches the reference point 1, the short-range behaviour of the spherically averaged conditional pair probability $P^{\sigma\sigma}_{\text{cond}}(\mathbf{r}, s)$ becomes of use. Here, $\mathbf{r}$ denotes the position of the reference point and s the radius of the sphere around $\mathbf{r}$. This can be described by a Taylor expansion:[65]

$$P^{\sigma\sigma}_{\text{cond}}(\mathbf{r}, s) = \frac{1}{3}\left(\tau_\sigma - \frac{1}{4}\frac{(\nabla\rho_\sigma)^2}{\rho_\sigma}\right)s^2 + ... \tag{7}$$

where the kinetic energy density τ_σ equals $\sum_i^\sigma |\nabla\phi_i|^2$.

$P^{\sigma\sigma}_{\text{cond}}(\mathbf{r}, s)$ does not only contain information about pair probability, but also about electron localization. Namely, if the probability of finding a second electron near the reference point is small, then the reference electron is more highly localized. The majority of information is contained in the leading term of the Taylor expansion:

$$D_\sigma = \tau_\sigma - \frac{1}{4}\frac{(\nabla\rho_\sigma)^2}{\rho_\sigma}. \tag{8}$$

As the relationship between electron localization and D_σ is inverse, i.e. small D_σ implies high localization, Becke and Edgecombe proposed an alternative formulation with more convenient features:

$$\text{ELF} = \left(1 + \chi^2_\sigma\right)^{-1}, \tag{9}$$

where $\chi_\sigma = D_\sigma / D_\sigma^0$ is a dimensionless localization index, calibrated with respect to the uniform electron gas using D_σ^0:

$$D_\sigma^0 = \frac{3}{5}\left(6\pi^2\right)^{2/3}\rho_\sigma^{5/3}. \tag{10}$$

D_σ^0 corresponds to the value that D_σ would take in a uniform electron gas with spin-density equal to the local value of $\rho_\sigma(\mathbf{r})$. The transformation of χ_σ into ELF using Eq. 9 restricts the possible values to the range $0 < \mathrm{ELF} \leq 1$, with $\mathrm{ELF} = 1$ corresponding to perfect localization and $\mathrm{ELF} = 1/2$ corresponding to localization identical to that in a uniform electron gas.

Savin and co-workers reinterpreted ELF in terms of kinetic energy[80] and proposed an alternative formulation for all electrons of the system regardless of their spin.[66] A further generalization was proposed by Kohout and Savin for spin-polarized systems.[67] This was adapted by Lu and Chen[68], leading to the ELF formulation that was used in this work:

$$\mathrm{ELF}(\mathbf{r}) = \frac{1}{1 + \left[D(\mathbf{r}) / D_0(\mathbf{r})\right]^2}, \tag{11}$$

where

$$\begin{aligned} D(\mathbf{r}) &= \frac{1}{2}\sum_i \eta_i \left|\nabla\phi_i(\mathbf{r})\right|^2 - \frac{1}{8}\left[\frac{\left|\nabla\rho_\alpha(\mathbf{r})\right|^2}{\rho_\alpha(\mathbf{r})} + \frac{\left|\nabla\rho_\beta(\mathbf{r})\right|^2}{\rho_\beta(\mathbf{r})}\right] \\ D_0(\mathbf{r}) &= \frac{3}{5}\left(6\pi^2\right)^{2/3}\left(\rho_\alpha^{5/3} + \rho_\beta^{5/3}\right). \end{aligned} \tag{12}$$

D. Berlin binding function

The Berlin binding function was originally introduced by Berlin to describe binding in diatomic molecules.[72] "Binding" differs from "bonding", in the sense that binding is related to the forces on the nuclei while bonding results from the energy of the molecule. Berlin proposed the following derivation to arrive at a function f, which divides the space into binding and anti-binding regions:[72]

For a diatomic molecule, the external force F required to keep the nuclei fixed at a distance R equals

$$F = -\frac{\partial E_e}{\partial R} = -\left\langle\frac{\partial V}{\partial R}\right\rangle = -\frac{\partial}{\partial R}\left\langle\frac{Z_1 Z_2 e^2}{R} - \sum_{i=1}^{N}\left(\frac{Z_1 e^2}{r_{1i}} + \frac{Z_2 e^2}{r_{2i}}\right) + \sum_{i<j}\frac{e^2}{r_{ij}}\right\rangle. \tag{13}$$

Since the inter-electronic distances r_{ij} are independent of R, we find that

$$\frac{\partial V}{\partial R} = -\frac{Z_1 Z_2 e^2}{R^2} + \sum_{i=1}^{N} \left(\frac{Z_1 e^2}{r_{1i}^2} \frac{\partial r_{1i}}{\partial R} + \frac{Z_2 e^2}{r_{2i}^2} \frac{\partial r_{2i}}{\partial R} \right). \tag{14}$$

resulting in

$$\begin{aligned} F &= \frac{Z_1 Z_2 e^2}{R^2} - \sum_{i=1}^{N} \int \cdots \int \phi_e^* \left(\frac{Z_1 e^2}{r_{1i}^2} \frac{\partial r_{1i}}{\partial R} + \frac{Z_2 e^2}{r_{2i}^2} \frac{\partial r_{2i}}{\partial R} \right) \phi_e d\tau_1 \ldots d\tau_N \\ &= \frac{Z_1 Z_2 e^2}{R^2} - \sum_{i=1}^{N} \int \left(\frac{Z_1 e^2}{r_{1i}^2} \frac{\partial r_{1i}}{\partial R} + \frac{Z_2 e^2}{r_{2i}^2} \frac{\partial r_{2i}}{\partial R} \right) \rho_i d\tau_i. \end{aligned} \tag{15}$$

Upon resolving the summation, the formula becomes

$$\begin{aligned} F &= \frac{Z_1 Z_2 e^2}{R^2} - \int \left(\frac{Z_1 e^2}{r_1^2} \frac{\partial r_1}{\partial R} + \frac{Z_2 e^2}{r_2^2} \frac{\partial r_2}{\partial R} \right) \rho d\tau \\ &= \frac{Z_1 Z_2 e^2}{R^2} - e^2 \int f \rho d\tau \end{aligned} \tag{16}$$

with

$$f = \left(\frac{Z_1}{r_1^2} \frac{\partial r_1}{\partial R} + \frac{Z_2}{r_2^2} \frac{\partial r_2}{\partial R} \right). \tag{17}$$

The sign of F determines the influence of the external forces on the molecule. When F is positive (negative), the external force prevents R from increasing (decreasing). The equilibrium value of R is reached when $F = 0$. As the electron density ρ is always positive at any point in space, the integral can be separated into regions depending on the sign of f:

$$F = \frac{Z_1 Z_2 e^2}{R^2} - e^2 \int_{f>0} f \rho d\tau - e^2 \int_{f<0} f \rho d\tau \tag{18}$$

It is now seen that an additional negative charge (i.e. an increase in ρ) can either cause F to

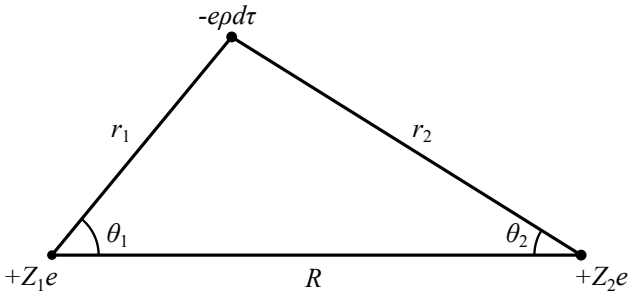

FIG. 1. Schematic representation of a diatomic molecule with relevant distances, angles and charges.

increase or decrease. In regions with positive f, increased density will cause the value of F to be reduced and the nuclei more tightly bound. The reverse occurs in regions with negative f. Consequently, the space is divided in a binding region ($f > 0$) and an anti-binding region ($f < 0$), separated by the surface formed by $f = 0$. This function f is now known as Berlin's function and should be regarded as a description of the binding force resulting from a unit negative charge.

For a diatomic molecule, it can be shown that $\partial r_1/\partial R = \cos\theta_1$ and $\partial r_2/\partial R = \cos\theta_2$, using the distances and angles as defined in Figure 1. The expression for f then becomes

$$f = \left(\frac{Z_1}{r_1^2}\cos\theta_1 + \frac{Z_2}{r_2^2}\cos\theta_2\right). \tag{19}$$

Wang and Peng extended the theoretical framework of the binding function to polyatomic molecules.[73] Their derivation starts from the geometric structure of a molecule with N nuclei, under the Born-Oppenheimer approximation. This is described by a generalized vector $\mathbf{R}$ containing all nuclear positions $\mathbf{R}_\alpha$:

$$\mathbf{R} = \{\mathbf{R}_1, \mathbf{R}_2, \ldots, \mathbf{R}_N\} = \left\{\sum_{\alpha=1}^{N}\frac{\mathbf{R}_1 - \mathbf{R}_\alpha}{N} + \sum_{\alpha=1}^{N}\frac{\mathbf{R}_\alpha}{N}, \quad \sum_{\alpha=1}^{N}\frac{\mathbf{R}_2 - \mathbf{R}_\alpha}{N} + \sum_{\alpha=1}^{N}\frac{\mathbf{R}_\alpha}{N}, \quad \ldots\right\}. \tag{20}$$

If the molecule is positioned such that the geometric centre is at the origin of the Cartesian coordinates, $\mathbf{R}$ is simplified to

$$\mathbf{R} = \left\{\sum_{\alpha=1}^{N}\frac{\mathbf{R}_1 - \mathbf{R}_\alpha}{N}, \quad \sum_{\alpha=1}^{N}\frac{\mathbf{R}_2 - \mathbf{R}_\alpha}{N}, \quad \ldots\right\}. \tag{21}$$

The binding function by Wang and Peng is based on the energy change occurring when all coordinates are scaled by the same scaling factor s. An increase in s implies totally symmetric stretching of the molecule, while a decrease implies shrinking. The new coordinates then become

$$\mathbf{R}_s = \left\{\sum_{\alpha=1}^{N} s\frac{\mathbf{R}_1 - \mathbf{R}_\alpha}{N}, \quad \sum_{\alpha=1}^{N} s\frac{\mathbf{R}_2 - \mathbf{R}_\alpha}{N}, \quad \ldots\right\}. \tag{22}$$

Wang and Peng defined their version of the binding function as

$$\begin{aligned} F_B(\mathbf{R}_0) &= \left(\frac{\partial E_s}{\partial s}\right)_{\mathbf{R}_0}\Bigg|_{s=1} = \left(\frac{\partial E_s}{\partial \mathbf{R}_s}\right)\cdot\left(\frac{\partial \mathbf{R}_s}{\partial s}\right)_{\mathbf{R}_0}\Bigg|_{s=1} \\ &= \sum_{\alpha=1}^{N} \mathbf{R}_\alpha \cdot \nabla_\alpha E \\ &= -\sum_{\alpha=1}^{N} \mathbf{R}_\alpha \cdot \mathbf{F}_\alpha \end{aligned} \tag{23}$$

where $\mathbf{R}_0$ denotes the original (unscaled) molecular coordinates.

It is now seen that the binding function equals the virial of the forces needed to hold all nuclei in the molecule fixed. The binding or anti-binding effect can be inferred from the sign of $F_B(\mathbf{R}_0)$: a positive $F_B(\mathbf{R}_0)$ indicates that the energy of the molecule increases when the molecule is stretched, meaning that the binding effect in the molecule is very strong. The reverse holds when $F_B(\mathbf{R}_0)$ is negative; the molecule experiences a strong anti-binding effect.

Eq. 23 can be further simplified, by using the equality $\mathbf{F}_\alpha = -\langle \nabla_\alpha V \rangle$ and following an analogous derivation as before (from Eq. 15 up till Eq. 16), so that

$$\begin{aligned} F_B(\mathbf{R}_0) &= \int \rho(\mathbf{r}) \cdot f_v d\mathbf{r} - \sum_{\alpha\neq\beta} \frac{Z_\alpha Z_\beta}{R_{\alpha\beta}} \\ &= \int_{f_v>0} \rho(\mathbf{r}) \cdot f_v d\mathbf{r} + \int_{f_v<0} \rho(\mathbf{r}) \cdot f_v d\mathbf{r} - \sum_{\alpha\neq\beta} \frac{Z_\alpha Z_\beta}{R_{\alpha\beta}}. \end{aligned} \tag{24}$$

The function f_v can again be used to separate the space into binding and antibinding parts. The expression

$$f_v = -\sum_{\alpha=1}^{N} \mathbf{R}_\alpha \cdot \frac{Z_\alpha \mathbf{r}_\alpha}{r_\alpha^3} \tag{25}$$

can be shown to be an exact description of the total binding effect resulting from the force generated by a unit charge.[73] In case the geometric centre of the molecule is not at the origin, the binding regions should be defined using a modified function

$$f_v' = f_v + \left(\sum_{\alpha=1}^{N} \frac{\mathbf{R}_\alpha}{N}\right) \cdot \sum_{\alpha=1}^{N} Z_\alpha \frac{\mathbf{r}_\alpha}{r_\alpha^3} \tag{26}$$

For a diatomic molecule, Eq. 25 simplifies to Berlin's definition of f (Eq. 19).

III. COMPUTATIONAL DETAILS

Electronic structure calculations were performed using the Q-Chem 5.4.1 software package.[81] Geometry optimizations and single-point energy calculations were performed at the ωB97M-V[82]/aug-cc-pVTZ[83,84] level of theory. Calculations on anionic species were performed at the optimized geometry of the corresponding neutral species. Explanations concerning the choice of functional and basis set, as well as the geometry optimization parameters can be found in our earlier work.[60] All nuclear charges were scaled to reach a total added charge of ΔZ a.u., corresponding to $\lambda = \Delta Z / Z_{\text{tot}}$, where Z_{tot} is the sum of the unmodified nuclear charges in the molecule expressed in a.u..

Electron localization functions were obtained from the Multiwfn software.[85] The formatted checkpoint files (fchk) obtained from the Q-Chem calculations described above were converted to extended wavefunctions files (wfx) using the conversion tool included in the AIMAll 19.10.12 package.[86] The resulting wfx files served as input for Multiwfn. For the calculation of α and β ELFs, the wfx input files were manually modified to contain only the information of α or β electrons, respectively. The grid spacing and extension distance were requested to be 0.1 and 10 bohr in each direction. Extrapolated electronic Fukui functions and ELFs were calculated as follows: For each grid point, a separate extrapolation procedure was carried out using the corresponding values of all ELFs calculated at different scaled nuclear charges. The intercept of the fitted quadratic curve was taken as value for the extrapolated ELF at that specific grid point. The data points included for extrapolation are listed in the SI. Values of the Berlin binding function were obtained by applying Eq. 26 to the optimized geometry of the neutral molecules.

IV. RESULTS AND DISCUSSION

A. Electronic Fukui functions and electron localization functions

For each molecule, we obtained the electronic Fukui function and four different ELFs, namely the total ELF for the neutral molecule, the total ELF for the anionic species, and the α and β ELFs for the anionic species. All of these, apart from the neutral ELF, have been obtained using the charge stabilization procedure. To our best knowledge, extrapolation of

spatial functions has not been reported before. On the contrary, the application of ELF to radical systems has already been studied.[69,70] Wherever possible, we compare with those results in order to establish that our extrapolated anion ELFs are reliable and useful for drawing conclusions. Furthermore, we investigate the relation between the total ELFs and the electronic Fukui functions, followed by a comparison of α and β ELFs to total ELFs.

1. Comparison of neutral and anion ELFs and Fukui functions

The electrophilic electronic Fukui function shows how the electron density changes upon addition of an electron. Regions of increasing density are most likely those where the additional electron is situated. ELF also provides a measure for situating the electrons, namely in those regions in space where the localization is high. These regions are called "basins", it is common to visualize them using the 0.8 a.u. isosurface. It was already shown that a visual comparison of neutral and anion ELF can assist in locating an excess electron.[69,70] Since the electronic Fukui function is calculated as the difference between electron densities of anion and neutral molecule, one could also calculate the same difference between electron localization functions. However, such "difference ELF" has thus far not been used, and it is not yet clear what the meaning and relevance are of this function.

We use the case of chloroethene for a detailed discussion. Figure 2 shows the electron localization functions for both the neutral molecule and the Π anion, as well as the difference between those ELFs together with the corresponding electronic Fukui function. By visually comparing the two ELFs, it is seen that the Π anionic ELF contains additional basins situated above and below the molecular plane. Furthermore, the basins corresponding to the carbon-carbon double bond and the carbon-hydrogen bond are now connected to each other. These changes with respect to the neutral ELF indicate the most likely localization of the excess electron. Upon looking at the difference ELF, it is confirmed that there is an increased localization in those regions. There are also regions exhibiting a decrease of localization, nevertheless the basins that were originally present in the neutral molecule are still retained in the anion.

Since the Fukui function is based on differences in densities, it does not contain much information about localization of the electrons. The regions of increased (decreased) localization are indeed also regions of increased (decreased) density, but the reverse is not always

true. For instance, there is a substantial density increase around the chlorine atom while the increase in localization is rather limited there. Thus, the analysis of ELFs agrees with the analysis of the Fukui function, and it contains the additional benefit of showing localization.

A similar analysis can be performed for the Σ anionic state of chloroethene. The relevant ELFs and Fukui function are shown in figure 3. Now, a large new basin is seen near the chlorine atom, as well as a small basin near the α hydrogen atom. The difference ELF confirms this and is in line with the Fukui function. Again, regions of increased (decreased) localization correspond to regions of increased (decreased) density but not vice versa. Furthermore, the anionic ELFs and difference ELFs confirm the Π and Σ character of the resonance states.

This analysis was repeated for the other studied compounds; the corresponding figures can be found in the SI. The results all showed the same trends: (i) Increased localization and electron density is found above and below the molecular plane for Π anions, and near the chlorine atom(s) for Σ anions. This is in line with the findings from our earlier work, in particular the atom-condensed electronic Fukui functions, from which we conclude that the calculated spatial functions are meaningful and thus that the extrapolation procedure is applicable. Moreover, in three of the studied compounds (*trans*-dichloroethene,

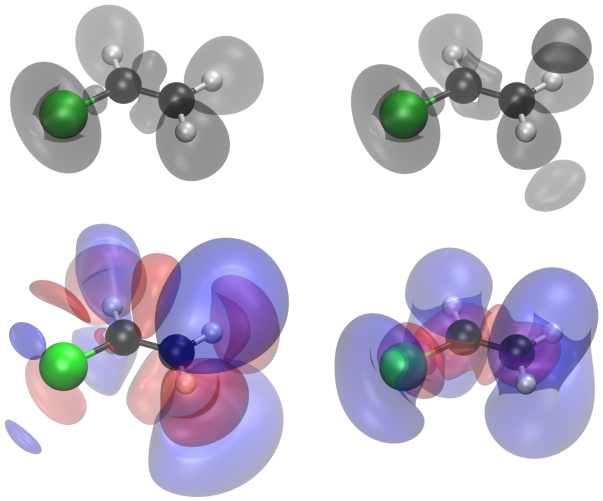

FIG. 2. Top row: Electron localization functions (isovalue 0.8 a.u.) for the neutral (left) and Π anionic (right) states of chloroethene. Bottom row: Difference ELF (left, isovalue 0.1 a.u.) and electronic Fukui function (right, isovalue 0.001 a.u) between the neutral and Π anionic state. Blue and red lobes represent positive and negative values, respectively.

1,1-dichloroethene and trichloroethene), the basins in the carbon-chlorine bond have decreased substantially in the anionic Σ state as compared to the neutral molecule. This is a first indication of bond weakining. (ii) Regions of increased (decreased) localization are also regions of increased (decreased) density, but not vice versa. (iii) The analysis of ELFs provides more information on top of the Fukui function. This last finding is in agreement with earlier reports of locating electrons by visually comparing ELFs.[69,70] The difference ELF however also proved to be useful, especially in cases when there were no large visual differences between the neutral and anion ELFs. An example of this is the ELF of the Σ anionic state of 1,1-dichloroethene (see figure 4). The neutral and anion ELF look extremely similar and the differences only become clear in the difference ELF, indicating increased localization near the chlorine atoms.

2. Comparison of α and β ELFs to total neutral and anion ELFs

We applied the method by Melin and Fuentealba[70] to calculate the α and β ELF using only the density and kinetic energy density resulting from α or β electrons, respectively. In reality, the unpaired electron can be of either α or β spin. By default in the software

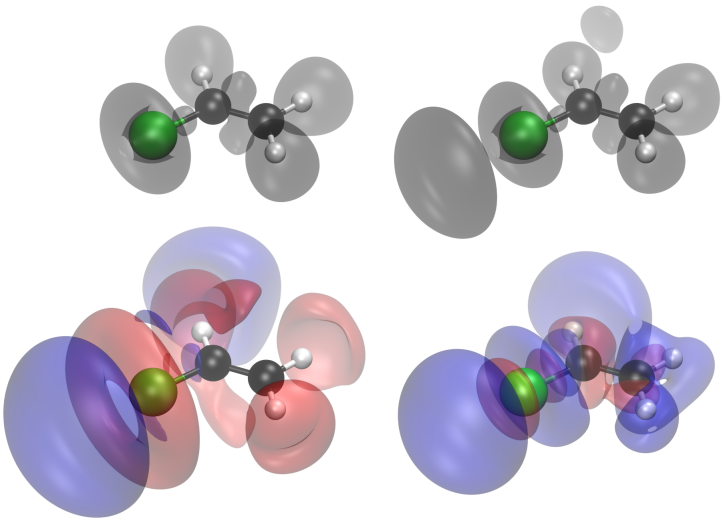

FIG. 3. Top row: Electron localization functions (isovalue 0.8 a.u.) for the neutral (left) and Σ anionic (right) states of chloroethene. Bottom row: Difference ELF (left, isovalue 0.1 a.u.) and electronic Fukui function (right, isovalue 0.001 a.u) between the neutral and Σ anionic state. Blue and red lobes represent positive and negative values, respectively.

we used, the unpaired electron in doublet DFT calculations is an α electron. It is thus expected that the α anionic ELF would be more similar to the total anionic ELF, and the β anionic ELF more similar to the total neutral ELF. The α ELF can be interpreted as an indication of where the unpaired electron is situated, regardless of its spin.[70] Figure 5 shows the total neutral ELF and three different Π anionic ELFs for chloroethene. As discussed before, the total anionic ELF contains additional basins as compared to the total neutral

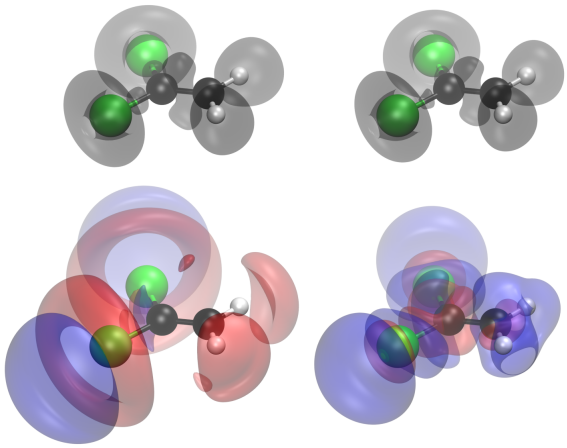

FIG. 4. Top row: Electron localization functions (isovalue 0.8 a.u.) for the neutral (left) and Σ anionic (right) states of 1,1-dichloroethene. Bottom row: Difference ELF (left, isovalue 0.1 a.u.) and electronic Fukui function (right, isovalue 0.001 a.u) between the neutral and Σ anionic state. Blue and red lobes represent positive and negative values, respectively.

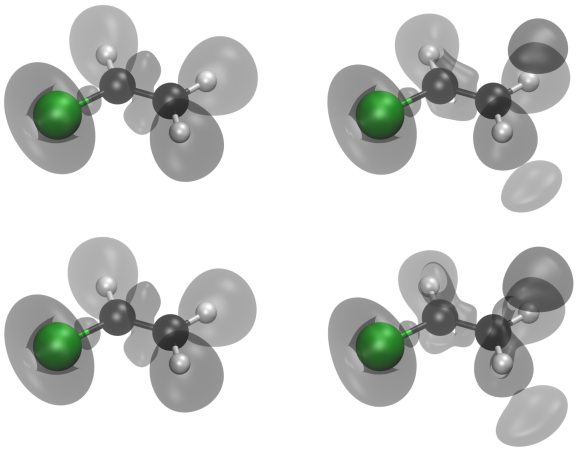

FIG. 5. Electron localization functions for chloroethene (neutral and Π anionic state, isovalue 0.8 a.u.). From top left to bottom right: neutral ELF, anion ELF, β anion ELF, α anion ELF.

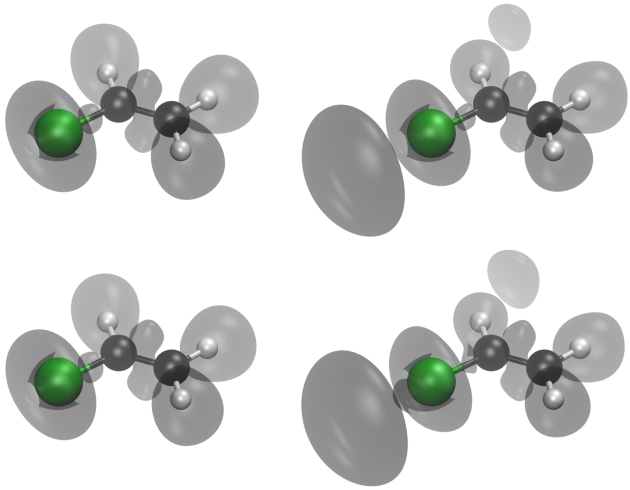

FIG. 6. Electron localization functions for chloroethene (neutral and Σ anionic state, isovalue 0.8 a.u.). From top left to bottom right: neutral ELF, anion ELF, β anion ELF, α anion ELF.

ELF. For chloroethene, these are two small basins above and below the molecular plane, and a connection between the carbon-carbon bond basin and the carbon-hydrogen bond basin. The same new basins are observed in the α anionic ELF, as expected. Contrarily, the β anionic ELF does not contain these and is more similar to the total neutral ELF. The same is observed for the Σ anionic ELFs of chloroethene (see Figure 6). As this agrees with reports on stable radicals, we can conclude that extrapolation yields accurate functions when applied to α and β ELFs. In cases where the total anionic ELF does not show the localization of the excess electron, the α anionic ELF can be employed. This is most visible

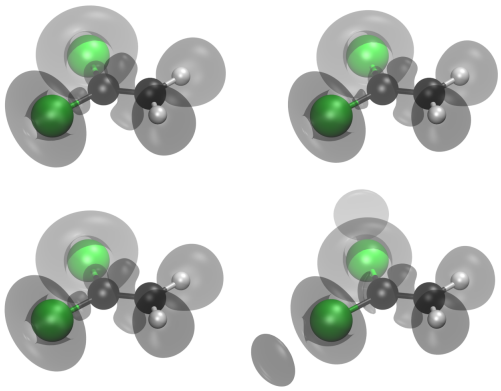

FIG. 7. Electron localization functions for 1,1-dichloroethene (neutral and Σ anionic state, isovalue 0.8 a.u.). From top left to bottom right: neutral ELF, anion ELF, β anion ELF, α anion ELF.

in the α Σ anionic ELF of 1,1-dichloroethene (Figure 7). The total anionic ELF does not show any additional basins, but they are visible in the α anionic ELF, close to the two chlorine atoms.

B. Electron localization functions and Berlin's binding functions

According to Berlin's theorem, addition of electron density in regions with positive BBF will cause the molecule to shrink, addition in regions with negative BBF will cause expansion and possibly bond breaking. Traditionally, BBF has thus been used in combination with electron densities or electronic Fukui functions in order to study the consequences of density changes for the molecular geometry. In the previous section, we showed that the ELF has an advantage because it provides a more informative measure of where the additional electron is localized. In combination with Berlin's binding function, this would lead to a more accurate idea of where the largest changes in the molecular geometry occur. We deem the extrapolated ELFs accurate enough for this kind of analysis, as concluded in the previous section. In the following, we apply the same reasoning as in Berlin's theorem, namely that new or enlarged ELF basins in regions with positive BBF will contribute to binding while those in regions with negative BBF will result in bond weakening. As far as we are aware, no other report of combining ELF and BBF has been published before, neither for bound nor for unbound electronic states

Fig. 8 shows BBF for all studied molecules. As the value of BBF only depends on the molecular geometry (see Eq. 26) and we use the same geometry for neutral and anionic states, it is the same for both states. The most notable regions of negative BBF are situated at the chloride atoms and extend away from the molecule. Above and below the molecular plane, BBF has a positive value. For the Π and Σ anionic states respectively, we thus anticipate that the new or enlarged ELF basins will be in a region with positive or negative BBF value respectively. This is verified by means of a combined visualization, by plotting a colored two-dimensional contour map of ELF and adding the BBF $= 0$ isocontour on top of it. One should be careful to choose a relevant plane for these plots. This plane should contain the most significant changes in ELF, being the new or enlarged basins. Again, we illustrate the procedure using the case of chloroethene. As mentioned before, the additional basins in the Π anionic state are located above and below the molecular plane. Hence it is a

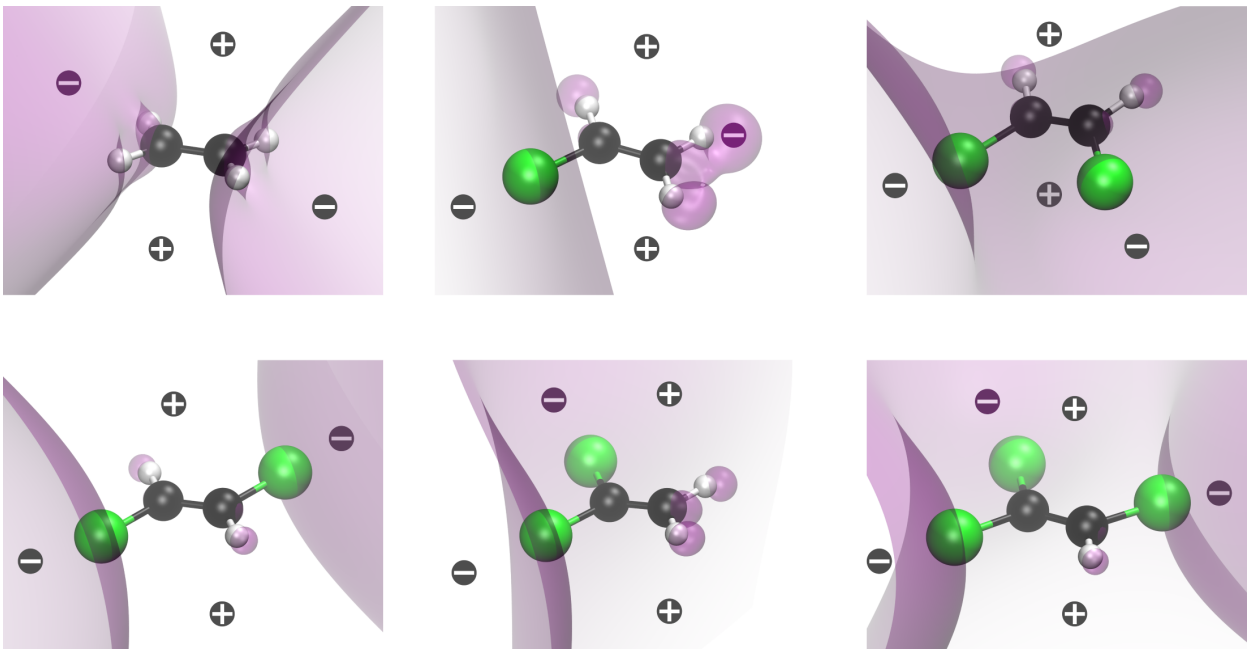

FIG. 8. Berlin's binding functions for the studied molecules (isovalue = 0 a.u.). From left to right: top row: ethene, chloroethene, *cis*-dichloroethene; bottom row: *trans*-dichloroethene, 1,1-dichloroethene, trichloroethene. Plus and minus signs indicate the sign of the functional values at either side of the plotted surface.

logical choice to plot the contours in the plane perpendicular to the molecule and containing the two carbon atoms. The result is shown in figure 9. Regions of high localization are those in light and dark blue. In both plots, the carbon atoms are very recognizable as the two small blue spheres in the centers of the figures, showing the core electrons. The double bond between them is visible as well. The white lines represent the BBF = 0 isocontour, the regions of positive and negative values are indicated by the plus and minus signs respectively. We can now see that the additional basins are located in a region of positive BBF, meaning that the excess electron will not contribute to molecule expansion or bond breaking.

For the Σ anionic state, the molecular plane is a good choice for plotting ELF and BBF, since this state is symmetric with respect to this plane and all additional or enlarged basins intersect it. Figure 10 shows the resulting plots. Again, the carbon atoms are recognizable as small blue spheres. The shell structure of the chlorine atom is also visible, whereas the hydrogen atoms appear as part of the σ bond with carbon. Of the new basins, a small one is present in a region of positive BBF and a large one in a region of negative BBF. These

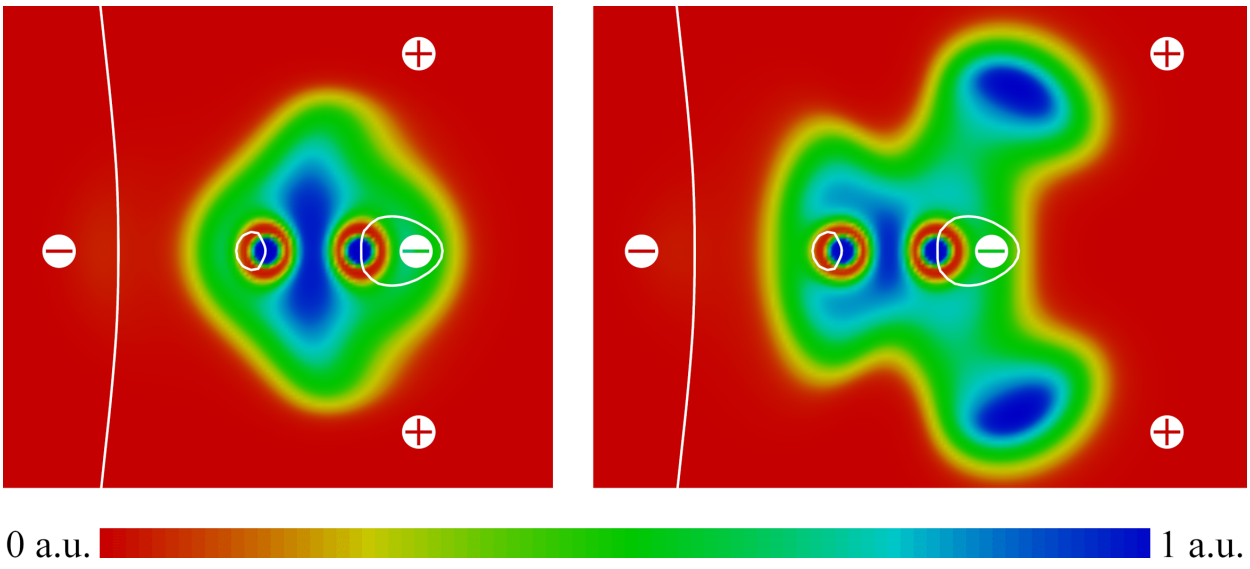

FIG. 9. Electron localization function (colored contours) and Berlin binding function (white contours) for the neutral (left) and Π anionic state (right) of chloroethene. The contours were plotted in the plane perpendicular to the molecular plane and containing the two carbon atoms.

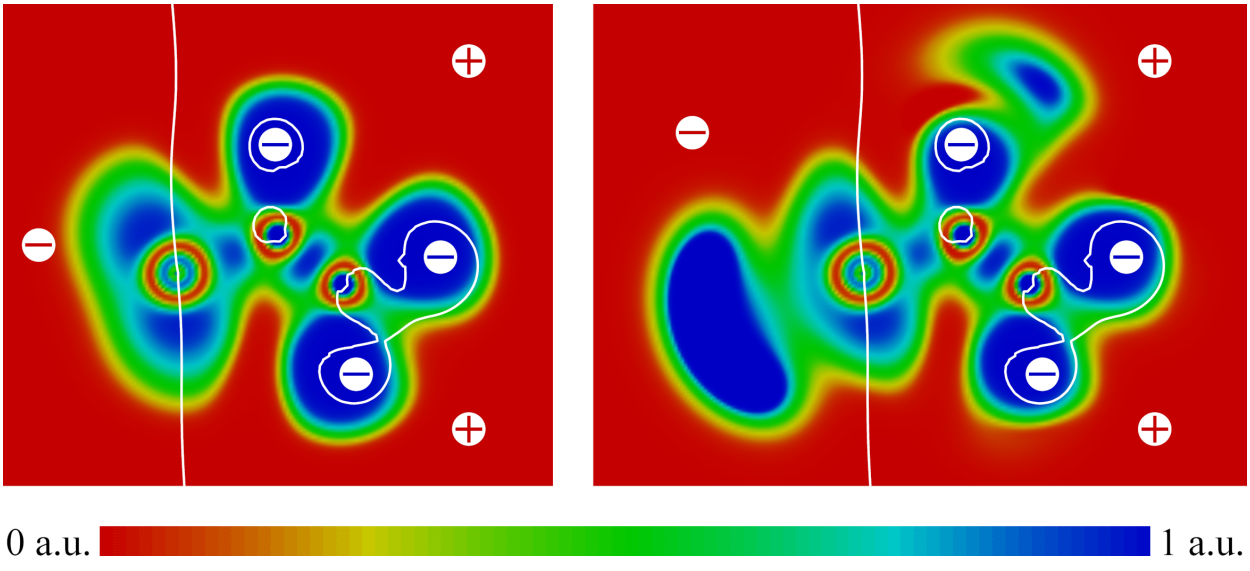

FIG. 10. Electron localization function (colored contours) and Berlin binding function (white contours) for the neutral (left) and Σ anionic state (right) of chloroethene. The contours were plotted in the molecular plane.

would cause both shrinking and enlarging of the molecule, however the enlarging effect would dominate. This enlarging effect would even be strongest on the carbon-chlorine bond. At this point, we can look back at the results from our earlier research.[60] We namely found that

there is a substantial stress on the carbon-carbon double bond in the Π anionic state, and large forces on the carbon-chlorine bond in the Σ anionic state. Based on the corresponding values, one could think that both resonance states could lead to bond breaking. For the Π state, this would correspond to breaking the carbon-carbon double bond. However, this had never been observed experimentally, and we had no theoretical means to explain why. Using our new results, we now have available the means to predict when and where DEA could happen. This enables us to better explain the experimental observations and use this knowledge to make predictions about the behavior of other electronic resonances for which experimental information is not (yet) available.

Analysis of the ELFs and BBFs for the other studied molecules (see figures in SI) shows that the same trends are valid: new or enlarged basins in the Π states are situated in regions with positive BBF, while those in the Σ states are situated in regions with negative BBF near the chlorine atom and will cause carbon-chlorine bond elongation.

V. CONCLUSIONS

We have extended the use of the charge stabilization method to spatial functions, namely the electronic Fukui function and the electron localization function. This was applied to the same set of metastable anions we studied before, namely the anions of ethene and the series of chloroethenes up to trichloroethene. The validity and usefulness of extrapolated spatial functions was demonstrated by comparison with results from other authors as well as our earlier results. The electron localization functions were shown to be a valuable tool for locating the excess electron in the metastable anion. For the first time, the difference ELF has been reported, which also proved to provide additional interesting information on the localization of the excess eelectron, especially in case the total neutral and anionic ELF do not differ much. Furthermore, the splitting into α and β ELFs was studied and compared to findings for stable radicals, from which we concluded that α and β ELFs are useful for metastable anions as well.

We also established a methodology for predicting the occurrence of dissociative electron attachment, by combining the electron localization function with Berlin's binding function. The results show that the Π anionic states are not dissociative but the Σ anionic states will lead to breaking of a carbon-chlorine bond. In future work, we hope to apply this method to

other compounds known to undergo DEA, especially those for which experiments are hard or impossible to perform. We also aim to combine conceptual DFT with non-Hermitian methods in order to avoid the need for an extrapolation procedure.

SUPPLEMENTARY MATERIAL

The coordinates of the optimized neutral compounds, an overview of the data points included for the extrapolation procedures, and all figures of electron localization functions and Berlin's binding functions can be found in the supplementary material.

ACKNOWLEDGMENTS

All authors wish to thank A. Savin for insightful discussions about ELF. C. T. thanks the Research Foundation-Flanders (FWO) for the received PhD fellowship (Grant No. 1103922N). T.-C. J. acknowledges funding from the European Research Council (ERC) under the European Union's Horizon 2020 research and innovation program (Grant/Agreement No. 851766), and the KU Leuven internal funds (grant C14/22/083). F. D. P. acknowledges the Strategic Research Program funding of the VUB. The displayed figures were created using VMD (for LinuxAMD64, version 1.9.4a51)[87] and GaussView 6.[88]

CONFLICTS OF INTEREST

The authors have no conflicts to disclose.

DATA AVAILABILITY

The data that support the findings of this study are available from the corresponding author upon reasonable request.

REFERENCES

[1]J. Simons, J. Phys. Chem. A 112, 29, 6401 (2008).

[2]I. I. Fabrikant, S. Eden, N. J. Mason, and J. Fedor, *Advances In Atomic, Molecular, and Optical Physics*, volume 66, pages 545–657, Academic Press (2017).

[3]P. Burrow, A. Modelli, N. Chiu, and K. Jordan, Chem. Phys. Lett. 82, 2, 270 (1981).

[4]P. J. Bruna, S. D. Peyerimhoff, and R. J. Buenker, Chem. Phys. Lett. 39, 2, 211 (1976).

[5]T.-C. Jagau, K. B. Bravaya, and A. I. Krylov, Annu. Rev. Phys. Chem. 68, 1, 525 (2017).

[6]N. Moiseyev, *Non-Hermitian Quantum Mechanics*, Cambridge University Press (2011).

[7]C. W. McCurdy and T. N. Rescigno, Phys. Rev. Lett. 41, 1364 (1978).

[8]G. Jolicard and E. J. Austin, Chem. Phys. Lett. 121, 1, 106 (1985).

[9]G. Jolicard and E. J. Austin, Chem. Phys. 103, 2, 295 (1986).

[10]U. V. Riss and H. D. Meyer, J. Phys. B: At., Mol. Opt. Phys. 26, 23, 4503 (1993).

[11]T.-C. Jagau, Chem. Commun. 58, 5205 (2022).

[12]S. Feuerbacher, T. Sommerfeld, and L. S. Cederbaum, J. Chem. Phys. 120, 7, 3201 (2004).

[13]Z. Benda and T.-C. Jagau, J. Chem. Theory Comput. 14, 8, 4216 (2018).

[14]Z. Benda and T.-C. Jagau, J. Phys. Chem. Lett. 9, 24, 6978 (2018).

[15]J. A. Gyamfi and T.-C. Jagau, J. Phys. Chem. Lett. 13, 36, 8477 (2022), pMID: 36054015.

[16]C. Titeca, F. De Proft, and T.-C. Jagau, J. Chem. Phys. 157, 21, 214106 (2022).

[17]B. Nestmann and S. D. Peyerimhoff, J. Phys. B: At., Mol. Opt. Phys. 18, 4, 615 (1985).

[18]R. G. Parr and W. Yang, J. Am. Chem. Soc. 106, 14, 4049 (1984).

[19]W. Yang and W. J. Mortier, J. Am. Chem. Soc. 108, 19, 5708 (1986).

[20]M. H. Cohen, M. V. Ganduglia-Pirovano, and J. Kudrnovský, J. Chem. Phys. 101, 10, 8988 (1994).

[21]A. D. Becke and K. E. Edgecombe, J. Chem. Phys. 92, 9, 5397 (1990).

[22]A. Savin, H.-J. Flad, J. Flad, H. Preuss, and H. G. von Schnering, Angew. Chem. Int. Ed. Engl. 31, 2, 185 (1992).

[23]M. Kohout and A. Savin, Int J Quantum Chem 60, 4, 875 (1996).

[24]T. Lu and F.-W. Chen, Acta Phys.-Chim. Sin. 27, 12, 2786 (2011).

[25]I. Fourré, B. Silvi, P. Chaquin, and A. Sevin, J Comput Chem 20, 9, 897 (1999).

[26]J. Melin and P. Fuentealba, Int J Quantum Chem 92, 4, 381 (2003).

[27]B. Silvi and A. Savin, Nature 371, 6499, 683 (1994).

[28]T. Berlin, J. Chem. Phys. 19, 2, 208 (1951).

[29]X. Wang and Z. Peng, Int J Quantum Chem 47, 5, 393 (1993).

[30]T. Koga, H. Nakatsuji, and T. Yonezawa, Journal of the American Chemical Society 100, 24, 7522 (1978).

[31]R. Balawender, F. De Proft, and P. Geerlings, J. Chem. Phys. 114, 10, 4441 (2001).

[32]D. Chakraborty, C. Cárdenas, E. Echegaray, A. Toro-Labbe, and P. W. Ayers, Chem. Phys. Lett. 539-540, 168 (2012).

[33]J. Horáček, I. Paidarová, and R. Čurík, J. Chem. Phys. 143, 18, 184102 (2015).

[34]T. Sommerfeld and M. Ehara, J. Chem. Phys. 142, 3, 034105 (2015).

[35]R. F. W. Bader and M. E. Stephens, J. Am. Chem. Soc. 97, 26, 7391 (1975).

[36]A. Savin, O. Jepsen, J. Flad, O. K. Andersen, H. Preuss, and H. G. von Schnering, Angew. Chem. Int. Ed. Engl. 31, 2, 187 (1992).

[37]E. Epifanovsky, A. T. B. Gilbert, X. Feng, J. Lee, Y. Mao, N. Mardirossian, P. Pokhilko, A. F. White, M. P. Coons, A. L. Dempwolff, Z. Gan, D. Hait, P. R. Horn, L. D. Jacobson, I. Kaliman, J. Kussmann, A. W. Lange, K. U. Lao, D. S. Levine, J. Liu, S. C. McKenzie, A. F. Morrison, K. D. Nanda, F. Plasser, D. R. Rehn, M. L. Vidal, Z.-Q. You, Y. Zhu, B. Alam, B. J. Albrecht, A. Aldossary, E. Alguire, J. H. Andersen, V. Athavale, D. Barton, K. Begam, A. Behn, N. Bellonzi, Y. A. Bernard, E. J. Berquist, H. G. A. Burton, A. Carreras, K. Carter-Fenk, R. Chakraborty, A. D. Chien, K. D. Closser, V. Cofer-Shabica, S. Dasgupta, M. de Wergifosse, J. Deng, M. Diedenhofen, H. Do, S. Ehlert, P.-T. Fang, S. Fatehi, Q. Feng, T. Friedhoff, J. Gayvert, Q. Ge, G. Gidofalvi, M. Goldey, J. Gomes, C. E. González-Espinoza, S. Gulania, A. O. Gunina, M. W. D. Hanson-Heine, P. H. P. Harbach, A. Hauser, M. F. Herbst, M. Hernández Vera, M. Hodecker, Z. C. Holden, S. Houck, X. Huang, K. Hui, B. C. Huynh, M. Ivanov, Á. Jász, H. Ji, H. Jiang, B. Kaduk, S. Kähler, K. Khistyaev, J. Kim, G. Kis, P. Klunzinger, Z. Koczor-Benda, J. H. Koh, D. Kosenkov, L. Koulias, T. Kowalczyk, C. M. Krauter, K. Kue, A. Kunitsa, T. Kus, I. Ladjánszki, A. Landau, K. V. Lawler, D. Lefrancois, S. Lehtola, R. R. Li, Y.-P. Li, J. Liang, M. Liebenthal, H.-H. Lin, Y.-S. Lin, F. Liu, K.-Y. Liu, M. Loipersberger, A. Luenser, A. Manjanath, P. Manohar, E. Mansoor, S. F. Manzer, S.-P. Mao, A. V. Marenich, T. Markovich, S. Mason, S. A. Maurer, P. F. McLaughlin, M. F. S. J. Menger, J.-M. Mewes, S. A. Mewes, P. Morgante, J. W. Mullinax, K. J. Oosterbaan, G. Paran, A. C. Paul, S. K. Paul, F. Pavošević, Z. Pei, S. Prager, E. I. Proynov, Á. Rák, E. Ramos-Cordoba, B. Rana, A. E. Rask, A. Rettig, R. M. Richard, F. Rob, E. Rossomme, T. Scheele, M. Scheurer, M. Schneider, N. Sergueev, S. M. Sharada, W. Skomorowski, D. W. Small, C. J. Stein,

Y.-C. Su, E. J. Sundstrom, Z. Tao, J. Thirman, G. J. Tornai, T. Tsuchimochi, N. M. Tubman, S. P. Veccham, O. Vydrov, J. Wenzel, J. Witte, A. Yamada, K. Yao, S. Yeganeh, S. R. Yost, A. Zech, I. Y. Zhang, X. Zhang, Y. Zhang, D. Zuev, A. Aspuru-Guzik, A. T. Bell, N. A. Besley, K. B. Bravaya, B. R. Brooks, D. Casanova, J.-D. Chai, S. Coriani, C. J. Cramer, G. Cserey, A. E. DePrince, R. A. DiStasio, A. Dreuw, B. D. Dunietz, T. R. Furlani, W. A. Goddard, S. Hammes-Schiffer, T. Head-Gordon, W. J. Hehre, C.-P. Hsu, T.-C. Jagau, Y. Jung, A. Klamt, J. Kong, D. S. Lambrecht, W. Liang, N. J. Mayhall, C. W. McCurdy, J. B. Neaton, C. Ochsenfeld, J. A. Parkhill, R. Peverati, V. A. Rassolov, Y. Shao, L. V. Slipchenko, T. Stauch, R. P. Steele, J. E. Subotnik, A. J. W. Thom, A. Tkatchenko, D. G. Truhlar, T. Van Voorhis, T. A. Wesolowski, K. B. Whaley, H. L. Woodcock, P. M. Zimmerman, S. Faraji, P. M. W. Gill, M. Head-Gordon, J. M. Herbert, and A. I. Krylov, J. Chem. Phys. 155, 8, 084801 (2021).

[38]N. Mardirossian and M. Head-Gordon, J. Chem. Phys. 144, 21, 214110 (2016).

[39]T. H. Dunning, J. Chem. Phys. 90, 2, 1007 (1989).

[40]D. E. Woon and T. H. Dunning, J. Chem. Phys. 98, 2, 1358 (1993).

[41]T. Lu and F. Chen, J Comput Chem 33, 5, 580 (2012).

[42]AIMAll (Version 19.10.12), Todd A. Keith, TK Gristmill Software, Overland Park KS, USA, 2019 (aim.tkgristmill.com).

[43]W. Humphrey, A. Dalke, and K. Schulten, J. Mol. Graph. 14, 1, 33 (1996).

[44]R. Dennington, T. A. Keith, and J. M. Millam, GaussView Version 6 (2019), semichem Inc. Shawnee Mission KS.

[45]J. Simons, J. Phys. Chem. A 112, 29, 6401 (2008).

[46]I. I. Fabrikant, S. Eden, N. J. Mason, and J. Fedor, *Advances In Atomic, Molecular, and Optical Physics*, volume 66, pages 545–657, Academic Press (2017).

[47]P. Burrow, A. Modelli, N. Chiu, and K. Jordan, Chem. Phys. Lett. 82, 2, 270 (1981).

[48]P. J. Bruna, S. D. Peyerimhoff, and R. J. Buenker, Chem. Phys. Lett. 39, 2, 211 (1976).

[49]T.-C. Jagau, K. B. Bravaya, and A. I. Krylov, Annu. Rev. Phys. Chem. 68, 1, 525 (2017).

[50]N. Moiseyev, *Non-Hermitian Quantum Mechanics*, Cambridge University Press (2011).

[51]C. W. McCurdy and T. N. Rescigno, Phys. Rev. Lett. 41, 1364 (1978).

[52]G. Jolicard and E. J. Austin, Chem. Phys. Lett. 121, 1, 106 (1985).

[53]G. Jolicard and E. J. Austin, Chem. Phys. 103, 2, 295 (1986).

[54]U. V. Riss and H. D. Meyer, J. Phys. B: At., Mol. Opt. Phys. 26, 23, 4503 (1993).

[55]T.-C. Jagau, Chem. Commun. 58, 5205 (2022).

[56]S. Feuerbacher, T. Sommerfeld, and L. S. Cederbaum, J. Chem. Phys. 120, 7, 3201 (2004).

[57]Z. Benda and T.-C. Jagau, J. Chem. Theory Comput. 14, 8, 4216 (2018).

[58]Z. Benda and T.-C. Jagau, J. Phys. Chem. Lett. 9, 24, 6978 (2018).

[59]J. A. Gyamfi and T.-C. Jagau, J. Phys. Chem. Lett. 13, 36, 8477 (2022), pMID: 36054015.

[60]C. Titeca, F. De Proft, and T.-C. Jagau, J. Chem. Phys. 157, 21, 214106 (2022).

[61]B. Nestmann and S. D. Peyerimhoff, J. Phys. B: At., Mol. Opt. Phys. 18, 4, 615 (1985).

[62]R. G. Parr and W. Yang, J. Am. Chem. Soc. 106, 14, 4049 (1984).

[63]W. Yang and W. J. Mortier, J. Am. Chem. Soc. 108, 19, 5708 (1986).

[64]M. H. Cohen, M. V. Ganduglia-Pirovano, and J. Kudrnovský, J. Chem. Phys. 101, 10, 8988 (1994).

[65]A. D. Becke and K. E. Edgecombe, J. Chem. Phys. 92, 9, 5397 (1990).

[66]A. Savin, H.-J. Flad, J. Flad, H. Preuss, and H. G. von Schnering, Angew. Chem. Int. Ed. Engl. 31, 2, 185 (1992).

[67]M. Kohout and A. Savin, Int J Quantum Chem 60, 4, 875 (1996).

[68]T. Lu and F.-W. Chen, Acta Phys.-Chim. Sin. 27, 12, 2786 (2011).

[69]I. Fourré, B. Silvi, P. Chaquin, and A. Sevin, J Comput Chem 20, 9, 897 (1999).

[70]J. Melin and P. Fuentealba, Int J Quantum Chem 92, 4, 381 (2003).

[71]B. Silvi and A. Savin, Nature 371, 6499, 683 (1994).

[72]T. Berlin, J. Chem. Phys. 19, 2, 208 (1951).

[73]X. Wang and Z. Peng, Int J Quantum Chem 47, 5, 393 (1993).

[74]T. Koga, H. Nakatsuji, and T. Yonezawa, Journal of the American Chemical Society 100, 24, 7522 (1978).

[75]R. Balawender, F. De Proft, and P. Geerlings, J. Chem. Phys. 114, 10, 4441 (2001).

[76]D. Chakraborty, C. Cárdenas, E. Echegaray, A. Toro-Labbe, and P. W. Ayers, Chem. Phys. Lett. 539-540, 168 (2012).

[77]J. Horáček, I. Paidarová, and R. Čurík, J. Chem. Phys. 143, 18, 184102 (2015).

[78]T. Sommerfeld and M. Ehara, J. Chem. Phys. 142, 3, 034105 (2015).

[79]R. F. W. Bader and M. E. Stephens, J. Am. Chem. Soc. 97, 26, 7391 (1975).

[80]A. Savin, O. Jepsen, J. Flad, O. K. Andersen, H. Preuss, and H. G. von Schnering, Angew. Chem. Int. Ed. Engl. 31, 2, 187 (1992).

[81]E. Epifanovsky, A. T. B. Gilbert, X. Feng, J. Lee, Y. Mao, N. Mardirossian, P. Pokhilko, A. F. White, M. P. Coons, A. L. Dempwolff, Z. Gan, D. Hait, P. R. Horn, L. D. Jacobson, I. Kaliman, J. Kussmann, A. W. Lange, K. U. Lao, D. S. Levine, J. Liu, S. C. McKenzie, A. F. Morrison, K. D. Nanda, F. Plasser, D. R. Rehn, M. L. Vidal, Z.-Q. You, Y. Zhu, B. Alam, B. J. Albrecht, A. Aldossary, E. Alguire, J. H. Andersen, V. Athavale, D. Barton, K. Begam, A. Behn, N. Bellonzi, Y. A. Bernard, E. J. Berquist, H. G. A. Burton, A. Carreras, K. Carter-Fenk, R. Chakraborty, A. D. Chien, K. D. Closser, V. Cofer-Shabica, S. Dasgupta, M. de Wergifosse, J. Deng, M. Diedenhofen, H. Do, S. Ehlert, P.-T. Fang, S. Fatehi, Q. Feng, T. Friedhoff, J. Gayvert, Q. Ge, G. Gidofalvi, M. Goldey, J. Gomes, C. E. González-Espinoza, S. Gulania, A. O. Gunina, M. W. D. Hanson-Heine, P. H. P. Harbach, A. Hauser, M. F. Herbst, M. Hernández Vera, M. Hodecker, Z. C. Holden, S. Houck, X. Huang, K. Hui, B. C. Huynh, M. Ivanov, Á. Jász, H. Ji, H. Jiang, B. Kaduk, S. Kähler, K. Khistyaev, J. Kim, G. Kis, P. Klunzinger, Z. Koczor-Benda, J. H. Koh, D. Kosenkov, L. Koulias, T. Kowalczyk, C. M. Krauter, K. Kue, A. Kunitsa, T. Kus, I. Ladjánszki, A. Landau, K. V. Lawler, D. Lefrancois, S. Lehtola, R. R. Li, Y.-P. Li, J. Liang, M. Liebenthal, H.-H. Lin, Y.-S. Lin, F. Liu, K.-Y. Liu, M. Loipersberger, A. Luenser, A. Manjanath, P. Manohar, E. Mansoor, S. F. Manzer, S.-P. Mao, A. V. Marenich, T. Markovich, S. Mason, S. A. Maurer, P. F. McLaughlin, M. F. S. J. Menger, J.-M. Mewes, S. A. Mewes, P. Morgante, J. W. Mullinax, K. J. Oosterbaan, G. Paran, A. C. Paul, S. K. Paul, F. Pavošević, Z. Pei, S. Prager, E. I. Proynov, Á. Rák, E. Ramos-Cordoba, B. Rana, A. E. Rask, A. Rettig, R. M. Richard, F. Rob, E. Rossomme, T. Scheele, M. Scheurer, M. Schneider, N. Sergueev, S. M. Sharada, W. Skomorowski, D. W. Small, C. J. Stein, Y.-C. Su, E. J. Sundstrom, Z. Tao, J. Thirman, G. J. Tornai, T. Tsuchimochi, N. M. Tubman, S. P. Veccham, O. Vydrov, J. Wenzel, J. Witte, A. Yamada, K. Yao, S. Yeganeh, S. R. Yost, A. Zech, I. Y. Zhang, X. Zhang, Y. Zhang, D. Zuev, A. Aspuru-Guzik, A. T. Bell, N. A. Besley, K. B. Bravaya, B. R. Brooks, D. Casanova, J.-D. Chai, S. Coriani, C. J. Cramer, G. Cserey, A. E. DePrince, R. A. DiStasio, A. Dreuw, B. D. Dunietz, T. R. Furlani, W. A. Goddard, S. Hammes-Schiffer, T. Head-Gordon, W. J. Hehre, C.-P. Hsu, T.-C. Jagau, Y. Jung, A. Klamt, J. Kong, D. S. Lambrecht, W. Liang, N. J. Mayhall, C. W. McCurdy, J. B. Neaton, C. Ochsenfeld, J. A. Parkhill, R. Peverati, V. A. Rassolov, Y. Shao, L. V. Slipchenko, T. Stauch, R. P. Steele, J. E. Subotnik, A. J. W. Thom, A. Tkatchenko, D. G. Truhlar, T. Van Voorhis, T. A. Wesolowski, K. B. Whaley, H. L.

Woodcock, P. M. Zimmerman, S. Faraji, P. M. W. Gill, M. Head-Gordon, J. M. Herbert, and A. I. Krylov, J. Chem. Phys. 155, 8, 084801 (2021).

[82]N. Mardirossian and M. Head-Gordon, J. Chem. Phys. 144, 21, 214110 (2016).

[83]T. H. Dunning, J. Chem. Phys. 90, 2, 1007 (1989).

[84]D. E. Woon and T. H. Dunning, J. Chem. Phys. 98, 2, 1358 (1993).

[85]T. Lu and F. Chen, J Comput Chem 33, 5, 580 (2012).

[86]AIMAll (Version 19.10.12), Todd A. Keith, TK Gristmill Software, Overland Park KS, USA, 2019 (aim.tkgristmill.com).

[87]W. Humphrey, A. Dalke, and K. Schulten, J. Mol. Graph. 14, 1, 33 (1996).

[88]R. Dennington, T. A. Keith, and J. M. Millam, GaussView Version 6 (2019), semichem Inc. Shawnee Mission KS.